Kinetic and Mechanistic Investigation of a Hydrolytic Catalytic Antibody Having Remarkable Substrate Specificity:[1] Substituent Effects on Catalysis

Yumiko Wada,*,# Masayoshi Yamamoto, Yukio Sudo, and Mitsunori Ono*,#

Research Laboratories, Ashigara, Fuji Photo Film Co., Ltd., Minami-Ashigara, Kanagawa 250-01

(Received July 9, 1998)

Monoclonal antibodies were raised against *p*-nitrophenyl phosphonate to elicit catalytic antibodies capable of hydrolyzing *p*-nitrophenyl carbonates. Of 34 clones selected, three clones catalyzed the hydrolysis of methyl *p*-nitrophenyl carbonate. Interestingly, 4A1, an antibody out of those clones, showed a significant rate acceleration against substrates that differ from the given haptenic structure in the carrier-proximal region. The rate acceleration (k_{cat}/k_{uncat}) for one of the specific substrates is 6.4×10^4, 20-fold higher than that of a substrate congruent with the hapten. Kinetic analysis of K_m and k_{cat} values, as well as the affinity constant (K_d) values of the corresponding transition-state analogs, indicated that the rate enhancement is associated with a decrease in the activation energy due to stabilization of the transition-state in the cleavage reaction. In addition, the inactivation of 4A1 catalytic antibody upon hydrolysis of a particular substrate was observed. The 600 MHz ^{13}C NMR measurement clearly showed that the ^{13}C-labeled fragment attached covalently to the 4A1 antibody, proving formation of an acyl-antibody. Further kinetic analysis study demonstrated that the 4A1 catalytic antibody uses a multistep kinetic sequence for the hydrolytic reaction.

Ever since Jencks's prediction[2] about the possibility of catalytic antibodies was demonstrated by two groups,[3,4] a variety of chemical transformations have been explored based on the concept of stereoelectronic complementarity in the transition-state.[5,6] The ability to select a catalytic antibody to any molecule of interest from more than 10^{12} possible antibodies makes the immune system an attractive source of specific catalysts.[7] One of the long-term goals is to find biocatalysts with substrate tolerance that offer potential applications to chemistry and biology.[8] Efforts have been made to expand the window for catalytic antibodies toward this end.[9—11] However, in most cases of immunization with a transition-state analog (hapten), the immune response has been driven to be homogeneous to the immunizing molecule, so that a strict homology of the substrate to the hapten is required for catalysis to take place.[4,12,13] Catalytic antibodies are thought, therefore, to permit little latitude in choice of substrate, although it is too early to conclude that the concept has practical limitations.[6,14]

In practice, when a catalytic antibody is elicited, three or four weak immunogenic methylene carbons are used to connect a hapten with a carrier protein in order to preclude steric interference from the carrier.[15,16] A substrate molecule location therefore can be separated into carrier-distal and carrier-proximal regions according to the corresponding hapten structure.[17]

The present work addresses the influence of substrate side chains on catalytic efficiency and specificity in antibody-driven hydrolysis.[18,19] This paper describes the enzymatic properties of a catalytic antibody 4A1, which shows a marked acceleration of hydrolysis of substrates differing in structure from the hapten in the carrier-proximal region. Kinetic studies revealed that this enhancement is not accompanied by a significant increase in K_m. In addition, the corresponding phosphate analogs exhibited affinity constants K_d with much lower values than that of the hapten. Therefore, we suggest that a specific affinity exists between the 4A1 catalytic antibody and the substrate side chain that lowers the activation energy in the cleavage reaction. In addition, successful detection of an acyl intermediate provides mechanistic understanding of a 4A1 catalytic antibody that involves a multistep kinetic sequence for the hydrolytic reaction.

Experimental

Synthesis of Hapten, Phosphates, and Carbonates. All the melting points were uncorrected. The homogeneity of each compound was checked by TLC over silica gel (Aldrich) with various solvent systems, and the spots were developed with cerium(IV) sulfate in dilute sulfuric acid. The IR and ^{1}H NMR (300 MHz) spectra were measured with Nujol and in chloroform-*d*, respectively, unless otherwise stated. ^{13}C NMR (600 MHz) was measured in D_2O. The abbreviations "s, d, t, dd, dt, q, m, and br" in the NMR spectra denote "singlet, doublet, triplet, double doublet, double triplet, quartet, mutiplet, and broad," respectively. The purification was carried out by flash column chromatography over silica gel 60 (240—400 mesh). Substrate **1a** and hapten **2a** were synthesized according to Shultz's procedure.[16] All other phosphates and substrates were prepared in accordance with the reported procedures referenced herein. Com-

Present address: Shionogi BioResearch Corp., 45 Hartwell Ave., Lexington, MA 02421-3102, USA.

mercially available chiral fragments were used as starting materials for the preparation of substrates **1d**, **1f**, and **1g**.

1a: Mp 90—92 °C. **1b**: Mp 95—100 °C; ^{1}H NMR δ = 2.08—2.25 (m, 2H), 2.37 (t, 2H, J = 8 Hz), 2.85 (d, 3H, J = 7 Hz), 4.36 (t, 2H, J = 8 Hz), 7.40, and 8.30 (ABq, each 2H, J = 11 Hz); IR 3400, 1780, 1660, 1630, 1600, 1530, and 1500 cm^{-1}, MS (FAB) *m/z* 283 (M+H). **1c**: Mp 54—56 °C; ^{1}H NMR δ = 1.43—1.85 (m, 4H), 3.50—3.70 (m, 1H), 4.20 (d, 2H, J = 7 Hz); IR 1760, 1610, 1590, 1510, 1490, 1280, 1200 cm^{-1}; MS (FAB) *m/z* 268 (M+H). (*S*)-**1d**: Mp 95—98 °C; $[\alpha]_D$ = +9.5 (*c* 0.87, $CHCl_3$); ^{1}H NMR δ = 1.35 (s, 3H), 1.45 (s, 3H), 3.65 (dd, 1H, J = 5.5 and 18 Hz), 3.75 (dd, 1H, J = 9 and 18 Hz), 4.25—4.35 (1H, m), 4.32 (dd, 1H, J = 4 and 10 Hz), 4.41 (dd, 1H, J = 6 and 10 Hz), 8.35 and 8.43 (ABq, each 2H, J = 5 Hz); IR 1780, 1610, 1570 cm^{-1}; MS (FAB) *m/z* 298 (M+H). (*R*)-**1d**: Mp 95—98 °C; $[\alpha]_D$ = +9.6 (*c* 0.87, $CHCl_3$). **1e**: Mp 80—83 °C; ^{1}H NMR δ = 5.40 (S, 2H), 7.2—7.6 (m, 5H), 8.25 and 8.42 (ABq, each 2H, J = 5 Hz), MS (FAB) *m/z* 274 (M+H). (*S*)-**1f**: Mp 128—130 °C; $[\alpha]_D$ = −35.4 (*c* 1.0, THF); ^{1}H NMR δ = 1.0 (t, 3H, J = 8 Hz), 1.42—1.75 (m, 2H), 2.08 (s, 3H), 4.12—4.41 (m, 3H), 5.80—6.0 (br, 1H, –NH), 7.40 and 8.30 (ABq, each 2H, J = 10 Hz); IR 3300, 1775, 1650, 1620, 1600, 1540 cm^{-1}; MS (FAB) *m/z* 297 (M+H). (*R*)-**1f**: Mp 128—130 °C; $[\alpha]_D$ = +35.2 (*c* 1.0, THF); MS (FAB) *m/z* 297 (M+H). (*S*)-**1g**: Mp 70—71 °C; $[\alpha]_D$ = +9.7 (*c* 1.0, $CHCl_3$); ^{1}H NMR ($CDCl_3$) δ = 1.98 (s, 3H), 2.91 and 2.96 (dd, each 1H, J = 9 and 6 Hz), 4.21 and 4.33 (dd, each 1H, J = 3 and 9 Hz), 4.50—4.62 (m, 1H), 5.71 (d, 1H, J = 5 Hz), 7.21—7.42 (m, 5H), and 8.27 and 8.31 (ABq, each 2H, J = 5 Hz); MS (FAB) *m/z* 359 (M+H). **^{13}C-labeled 1g**: Mp 72 °C; $[\alpha]_D$ = +10.0 (*c* 1.0, $CHCl_3$); ^{1}H NMR ($CDCl_3$) δ = 1.95 (d, 3H, J(C–H) = 7 Hz), 2.92 and 2.96 (dd, each 1H, J = 9 and 6 Hz), 4.20 and 4.32 (dd, each 1H, J = 3 and 9 Hz), 4.45—4.68 (m, 1H), 5.22—5.40 (br, 1H), 7.12—7.38 (m, 5H), and 7.98 and 8.28 (ABq, each 2H, J = 5 Hz); MS (FAB) *m/z* 360 (M+H). **2a**: Mp > 200 °C (decomp); MS (FAB) *m/z* 302 (M − Na). **2b**: Mp > 200 °C; ^{1}H NMR (DMSO-d_6) δ = 3.46 (s, 3H, $-OCH_3$); IR 1615, 1550, 1340, 1200, 1150 cm^{-1}; MS (FAB) *m/z* 232 (M − Na). **2c**: Mp > 200 °C; IR 1610, 1595, 1400, 1320, 1155 cm^{-1}; MS (FAB) *m/z* 302 (M − Na). **2d**: Mp > 200 °C; IR 1620, 1605, 1580, 1300, 1190, 1185 cm^{-1}; MS (FAB) *m/z* 332 (M − Na). **2e**: Mp > 200 °C; ^{1}H NMR (DMSO-d_6) δ = 4.94 (s, 2H, $-CH_2-$), 7.32—7.86 (m, 5H); MS (FAB) *m/z* 308 (M − Na). **2f**: Mp > 200 °C; ^{1}H NMR (DMSO-d_6) δ = 3.39 (br s, 2H), 4.95 (br s, 2H), 7.42—7.88 (m, 5H); MS (FAB) *m/z* 322 (M − Na). **2g**: Mp > 200 °C; ^{1}H NMR (DMSO-d_6) δ = 1.72 (dt, 2H, J = 6.5 and 7.0 Hz), 2.49 (t, 2H, J = 6.5 Hz), 3.82 (br t, 2H, J = 7.0 Hz); MS (FAB) *m/z* 336 (M − Na).

Preparation of Conjugates and Monoclonal Antibody Production. Hapten **2a** (0.1 mmol) was coupled to the carrier proteins, keyhole limpet hemocyanin (KLH) and BSA (1.3 μmol), using 1-[3-(dimethylamino)propyl]-3-ethylcarbodiimide (0.5 mmol) in 30 mM NaCl at pH = 7.5—8.0 (1 M = 1 mol dm^{-3}). Epitope densities of 14 and 13 for KLH and BSA, respectively, were determined by alkaline hydrolysis of the conjugates at 90 °C for 20 min in 1 M NaOH. Balb/c mice were immunized with the KLH-hapten conjugate (20 μg) emulsified in complete Freund's adjuvant. After additional immunizations for 6 months (20 μg each time in incomplete Freund's adjuvant), a boost (20 μg in PBS) was subcutaneously administered, and 3 d later the spleen cells were fused with Sp2 myeloma cells. The hybridoma supernatants were screened for binding to the BSA–hapten conjugate using ELISA.

Thirty-four monoclonal immunoglobulin G (IgG) antibodies were purified from ascitic fluid by Protein A-Sepharose 4B affinity chromatography eluted by pH gradient. The homogeneity of the antibodies was judged to be greater than 95% by SDS polyacrylamide gel electrophoresis. The subclass was determined to be IgG2a for 4A1 and to be IgG1 for 1G2 and 5H2.

Hydrolysis Assay. The release of *p*-nitrophenol was monitored at 400 nm by a Hitachi 2284 double beam spectrophotometer. Substrates, in tetrahydrofuran (THF) stock solution, were diluted with 10 mM Tris/HCl (pH 8.5), and added to the antibody; the final THF concentration was 2%. The concentration of antibody was 4.4 μM, and the concentration of substrates ranged from 50 to 1000 μM. The background rate was determined by extrapolation of the rate of the uncatalyzed reaction, under the same conditions, to zero buffer concentration.[16] The apparent K_i value for 4A1 antibody was estimated by fitting initial rate data to the equation for tight-binding inhibition:

$v = v_0/(2\alpha E)\{[(K_i+I-\alpha E)^2+4K_i\alpha E]^{1/2}-(K_i+I-\alpha E)\}$, where v and v_0 is the initial rate in the presence or absence of inhibitor, respectively, αE represents the fractional (α) concentration of functional antibody binding sites (E), I is the concentration of inhibitor, and K_i is the apparent inhibition constant.[20] The substrate concentration used for estimation of the apparent K_i was 800 μM. The value was confirmed at substrate concentrations of 600 μM. The antibody concentration was fixed at 4.4 μM. Data were fit to the equation using the nonlinear estimation module of STATISTICA from StatSoft, Inc. (Tulsa OK, USA).

Competitive ELISA. The apparent affinity constants (K_d) of **2a—2g** were determined by competitive ELISA procedure using BSA-hapten conjugate.[21] The concentration of antibody was 1.3 nM, and the apparent competitive inhibition assay was performed at ten different concentrations of inhibitors with a range from 1×10^{-9} to 1×10^{-1} M.

Quantitation of Phenylalaninol. HPLC analysis of (*S*)-(−)-*N*-acetylphenylalaninol (2-acetylamino-3-phenyl-1-propanol) was performed using a YMC-Pack reverse-phase column eluted with a linear gradient of 0—100% aqueous CH_3CN at pH 7.5. Under this condition, a peak at retention time of 16.2 min was found to be identical with a peak of (*S*)-(−)-*N*-acetylphenylalaninol, mp 128 °C; $[\alpha]_D$ = +23, by direct comparison with an authentic sample.

pH-Rate Profiles. The 4A1-catalyzed hydrolysis of substrate **1a** was measured at different pH values in the range 7.5 to 9.5 using two buffer systems (10 mM Tris/HCl at pH 7.5—9.0; 10 mM H_3BO_3/Na_2CO_3 at pH 8.0—9.5). A plot of $\log k_{cat}$ vs. pH exhibited a linear relationship in the range tested in both buffer systems. The K_m value for substrate **1a** did not vary significantly in the pH range 7.5 to 9.5. Because another study also showed that catalytic antibodies display maximum activity (k_{cat}) at pH 10.5, irreversible denaturation of the antibody can be negligible in this lower pH range.[22]

Incorporation of [^{13}C]-Labeled *N*-Acetylphenylalaninol. Carbonate **1g** (5 mM) labeled with ^{13}C on the *N*-acetyl carbonyl carbon was reacted with 4A1 antibody (73 μM) for 1 h at 30 °C and pH 8.5. The reaction mixture then was extensively dialyzed with D_2O containing 150 mM NaCl at 4 °C for 24 h.

Results

Enzymatic Properties of Catalytic Antibodies. Antibodies were raised against *p*-nitrophenyl phosphonate **2a** linked by four methylene carbons with carrier protein to elicit catalytic antibodies capable of hydrolyzing *p*-nitrophenyl carbonates.[16] Of 34 clones selected, three clones catalyzed the hydrolysis of methyl *p*-nitrophenyl carbonate **1a**. The k_{cat} and K_m values for the three catalytic antibodies

were determined from Lineweaver–Burk plots (Tables 1 and 2). Two antibodies (1G2 and 5H2) catalyzed the reaction on the order of several hundred-fold over the uncatalyzed rate; however, antibody 4A1 was the most efficient catalyst with a value of k_{cat}/k_{uncat} of 3.0×10^3 at pH 8.5. The pH profile on 4A1-catalyzed hydrolysis of **1a** over a pH range of 7.5 to 9.5 revealed that the k_{cat} exhibits a first-order dependence on hydroxide ion concentration in the pH range (Fig. 1). The antibody-catalyzed reactions were completely inhibited by hapten **2a** and a "short" transition-state analog, phosphate **2b**, proving that the catalytic activity is associated with binding at the antibody-combining site. The K_i values of phosphate **2b** for 1G2 and 5H2 were 15 and 40 μM at 30 °C, respectively. In the case of 4A1, only 20% of the binding activity of the antibody treated by phosphate **2b** was recovered after 3 d of extensive dialysis at 4 °C. Initial rate data measured at increasing concentrations of phosphate **2b** in 4A1 catalyzed hydrolysis of **1a** were fit to the equation for tight-binding inhibition, as described in the Experimental Section. The estimated apparent K_i value was 43 nM.

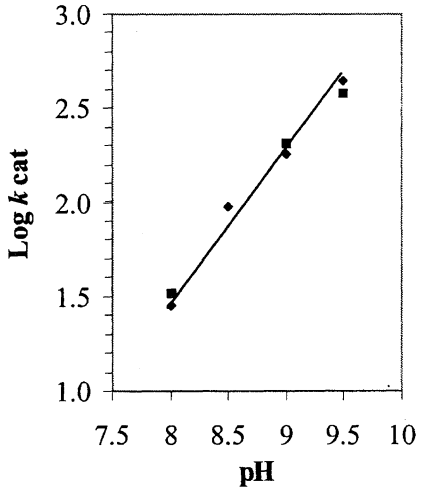

Fig. 1. pH rate profile for 4A1 catalyzed hydrolysis of substrate **1a**. The antibody concentrations were 4.4 μM (◆) and 0.88 μM (■).

Structural Influence of the Carrier-Proximal Region. In order to assess geometric and electronic influences on the carrier-proximal region in the substrate, several derivatives were designed and synthesized, as shown in Fig. 2. Experiments using 4A1 catalytic antibody were repeated three times for each substrate; the kinetic parameters in the hydrolysis were then calculated as shown in Table 2. Substrate **1b**, having the same carbon linkage as the hapten, showed almost the same catalytic efficiency (k_{cat}/k_{uncat} of 3700) as that of a truncated substrate **1a** in which the linking portion was ignored, whereas 4A1 substantially accelerated the hydrolysis of substrates **1c, 1d, 1e**, and **1f** (k_{cat}/k_{uncat} of 8000, 30000, 5200, and 6000, respectively, at pH 8.5; see Table 2). It should be noted that these substrates have spatially extended substituents different from the inducing hapten in the carrier-proximal region. This property of 4A1 is important, because the other two catalytic antibodies (1G2 and 5H2) elicited from the same immunization afforded negligible rate enhancement against these substrates (such as **1d**, shown in Table 1). According to the results of thermodynamic studies

Table 1. Kinetic Parameters for the Hydrolysis of Substrate **1a** and **1d** by Catalytic Antibodies
All parameters were determined at 30 °C in 98% Tris/HCl pH 8.5 and 2% THF in the presence or absence of antibody (4.4 μM).

Catalytic antibody	Substrate **1a**			Substrate **1d**		
	K_m / μM	K_{cat} / min^{-1}	k_{cat}/k_{uncat}	K_m / μM	K_{cat} / min^{-1}	k_{cat}/k_{uncat}
1G2	749	1.6	440	837	1.4	260
5H2	477	1.7	450	403	1.3	240
4A1	641	12.7	3000	528	122	30000

Table 2. Summary of the Kinetic Parameters for 4A1 Antibody Catalyzed Reactions
The kinetic parameters were determined at 30 °C in 98% Tris/HCl pH 8.5 and 2% THF in the presence or absence of antibody (4.4 μM).

Substrate	K_m / μM	K_{cat} / min^{-1}	K_{uncat} / min^{-1}	k_{cat}/k_{uncat}	k_{cat}/k_{uncat} / $min^{-1}\,\mu M^{-1}$
1a	641	13	0.0044	3000	0.02
1b	238	13	0.0035	3700	0.02
1c	547	30	0.0038	8000	0.05
1d	528	122	0.0035	30000	0.23
1e	470	21	0.0040	5200	0.03
(***S***)-**1d**	586	224	0.0035	64000	0.38
(***R***)-**1d**	363	50	0.0035	14000	0.14
(***S***)-**1f**	812	23	0.0038	6000	0.03
(***R***)-**1f**	607	9	0.0035	2400	0.01

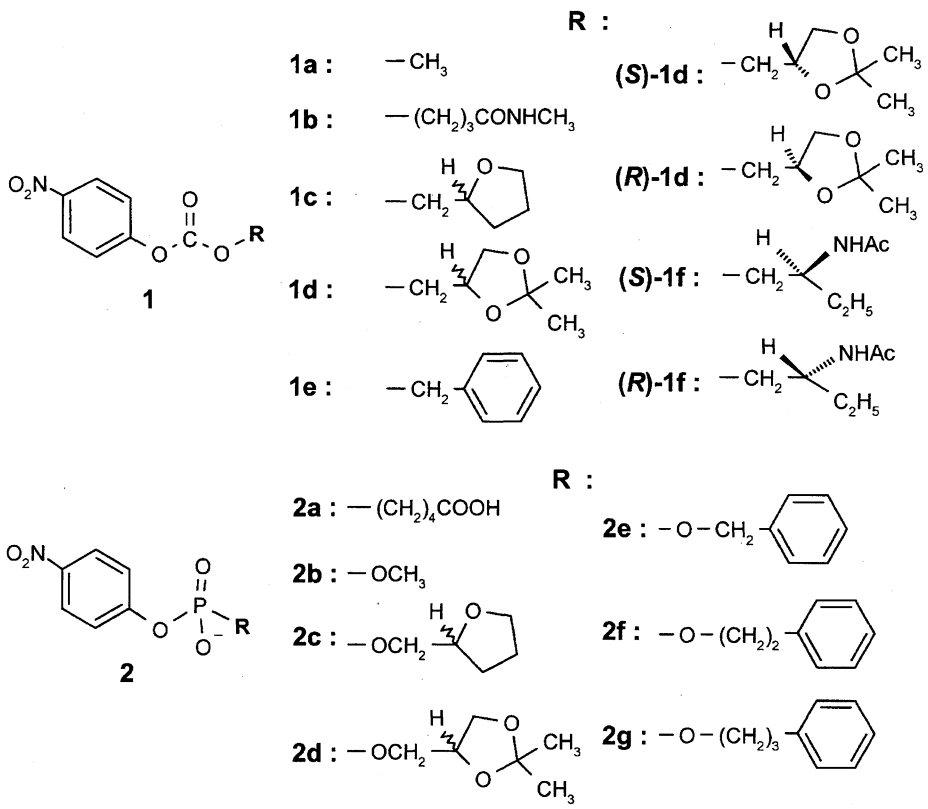

Fig. 2. Structures of substrates **1a**—**1f**, phosphonate (hapten) **2a**, and phosphates (transition-state analogs) **2b**—**2g**. **1c, 1d, 2c**, and **2d** denote the racemates.

(Fig. 3), the apparent K_d value of phosphate **2d**, a transition-state analog of **1d**, was 6.2×10^{-7} M, demonstrating that 4A1 catalytic antibody has a much higher affinity with phosphate **2d** than with hapten **2a** ($K_d = 2.5\times10^{-5}$ M). The relative importance of structural features affecting the hydrolytic activity of 4A1, could be assessed by the kinetic parameters summarized in Table 2. The results indicated that the potential substrates bear a branch at the β-carbon vicinal to the α-methylene group (i.e., **1c—1f**), proton-accepting groups such as ether oxygen (i.e., **1c, 1d**) or carbonyl oxygen (i.e., **1f**). Besides, the benzene ring in substrate is not playing a crucial role for a strong interaction with 4A1 binding site, we can so conclude by considering the rate enhancement for **1e**, in addition to the moderate binding constants $K_d = 1.6\times10^{-5}$ M, 1.0×10^{-5} M, and 1.5×10^{-5} M for the transition-state analogs **2e, 2f**, and **2g**, respectively.

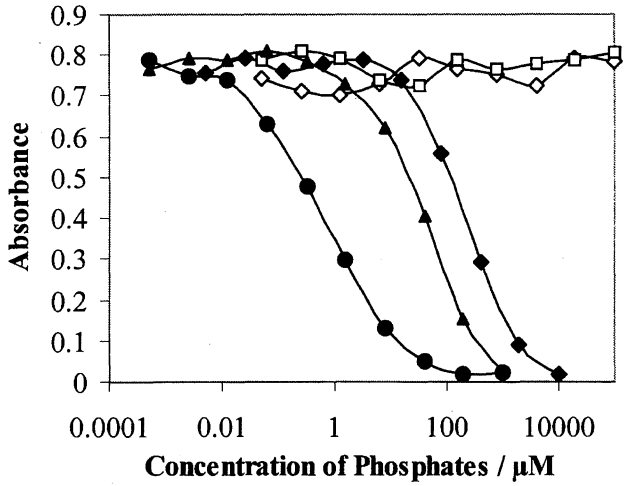

Fig. 3. Competitive ELISA. The apparent affinity constants (K_d) of 4A1 catalytic antibody for transition state analogs were determined by using BSA–hapten conjugates: ▲; hapten **2a**, ◆; a short transition state analog **2b**, ●; **2d**, □; phenylalaninol **3**, ◇; *p*-nitrophenol **4**.

Effect of Chirality in the Substrate. Each enantiomer of **1d** and **1f** was separately synthesized and tested in hydrolytic reaction with 4A1. As shown in Table 2, 4A1 antibody preferably catalyzed the enantiomer with an *S* configuration in both substrates **1d** and **1f** ($k_{cat}/k_{uncat} = 6.4\times10^4$ and 6.0×10^3, respectively), rather than the corresponding enantiomer with an *R* configuration. Although the enantioselectivity is modest ($k^S_{cat}/k^R_{cat} = 4.5$ and 2.5, respectively), the rate differential indicates clearly that the chiral environment of the 4A1 combining site discriminates between the two enantiomerically different transition-states.[23] It is interesting to note that the antibody was elicited by hapten **2a** without any chiral element.[24,25]

Detection of an Acyl Intermediate. Substrate **1g** (200 μM), which possessed a benzyl moiety instead of an ethyl group (as in (*S*)-**1f**), was hydrolyzed by 4A1 (4.4 μM) at 30 °C in 10 mM Tris/HCl buffer at pH 8.5. After the initial burst, a steep retardation occurred and then the liberation of *p*-nitrophenol was saturated, as shown in Fig. 4. Catalytic activity was not recovered even after extensive dialysis at

pH 3.0 in citrate buffer. In addition, this inactivation caused complete loss of binding affinity for the hapten. However, when the inactivated 4A1 was incubated in 10% aqueous CH_3CN at 37 °C at pH 10.5 for 1 h after dialysis, more than 93% of the catalytic activity for (*S*)-**1d** and the binding affinity for hapten were recovered in the 4A1 antibody. After the treatment at pH 10.5, followed by ultracentrifugation, a fragment of (*S*)-(−)-*N*-acetylphenylalaninol **3**, not *p*-nitrophenol **4**, was detected by HPLC analysis of the reaction solution. The released fragment **3** was quantitated as 1.85 molecules per antibody. The competitive ELISA showed that neither phenylalaninol **3** nor *p*-nitrophenol **4** is able to inhibit 4A1 catalytic antibody from binding to the hapten (Fig. 3).

^{13}C-labeled substrate **1g** on the *N*-acetyl carbonyl carbon was synthesized and given into the same inactivation experiment with 4A1 in D_2O. A solution of the concentrate was then measured by 600 MHz ^{13}C NMR. The resulting spectrum clearly indicated the ^{13}C-enriched carbonyl carbon peak at 176.2 ppm in D_2O, which can be assigned to (*S*)-(−)-*N*-acetyl carbonyl carbon (Fig. 5). This was identical with results obtained by direct comparison of the chemical shift in CD_3OD of an authentic sample of ^{13}C-labeled *N*-acetylphenylalaninol.

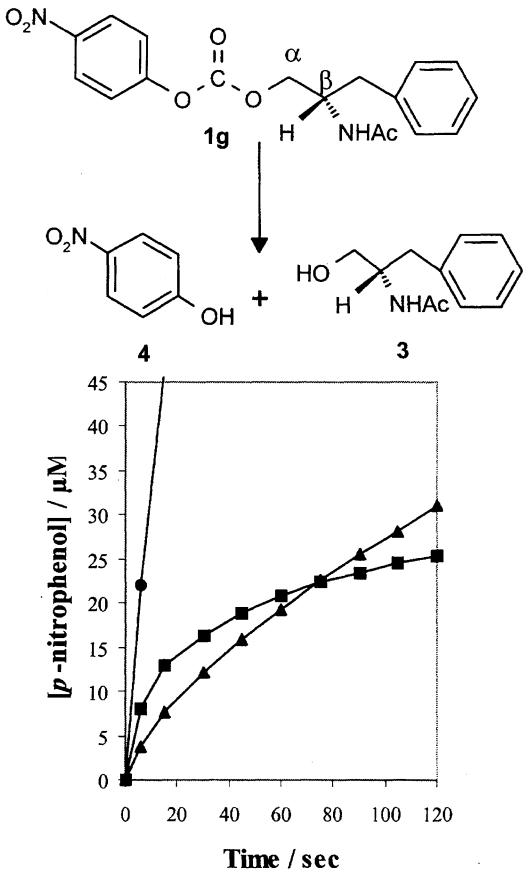

Fig. 4. Inactivation of 4A1 catalytic antibody upon hydrolysis of substrate **1g**. All reactions were carried out by use of 4A1 antibody (4.4 μM) and substrates (200 μM), ■; **1g**, ●; (*S*)-**1d**, ▲; **1a**. Substrate, in THF stock solution, were diluted with 10 mM Tris/HCl, and added to the antibody.

Discussion

This study revealed a remarkable property of a catalytic antibody; i.e., it accelerates the hydrolytic reaction of carbonates that differ from a given haptenic structure in the carrier-proximal region. Because this catalytic antibody also showed the most efficient catalytic efficiency against a truncated substrate **1a** that consists only of the carrier-distal and immunogenic regions, it provides an interesting opportunity to analyze a pattern of specificity and efficiency in 4A1 catalytic antibody given by the enormous diversity of the immune system.

The 4A1-catalyzed reaction exhibited a first-order dependence on hydroxide ion concentration, whereas the K_m was relatively unaffected, at pH values ranging from 7.5 to 9.5. This suggests that the hydroxide ion may be directly attacking either the polarized carbonyl of the Ig-complexed substrate or a covalently attached acyl intermediate.[26] Fortunately, the discovery of inactivation of 4A1 antibody brought about by substrate **1g** hydrolysis led to our further understanding of the reaction mechanism. Complete recovery of the 4A1 antibody's catalytic activity was observed after treatment of the inactivated 4A1 antibody at high pH (ca. 10.5), but not at low pH (ca. 3.5). Although *p*-nitrophenol was not detected in the reaction solution treated at pH 10.5, the side chain (fragment **3**) of substrate **1g** was detected by HPLC. It was calculated to be 1.85 molecules per one molecule of antibody; hence the stoichiometric amount of the side chain of substrate **1g** at the binding site is thought to prevent the catalysis. In addition, the competitive ELISA demonstrated that fragment **3** itself does not bind to 4A1 ($K_d > 0.1$ M). Therefore the inactivation of 4A1 resulting from reaction with **1g** is not due to product inhibition. The weak binding of fragment **3** suggests instead that 4A1 incorporates the side chain of the substrate during the hydrolytic reaction process.[21] The ^{13}C NMR study also

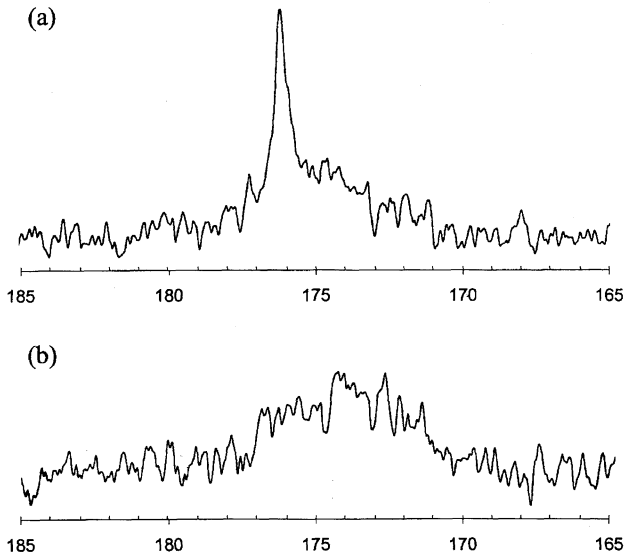

Fig. 5. 600 MHz ^{13}C NMR spectra of fragment **3** incorporated 4A1 (a) and intact 4A1 (b).

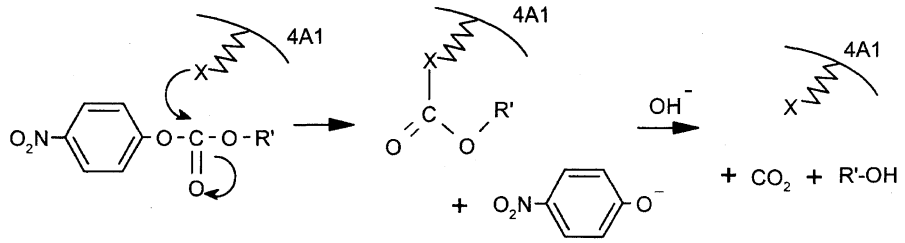

Fig. 6. A scheme of 4A1 antibody catalyzed hydrolysis. The reaction is most likely mediated by acyl-antibody intermediate resulting from nucleophilic attack by amino acid residue in or near the combining site. X: amino acid residue.

clearly showed the existence of covalently attached fragment **3** on 4A1 antibody. The inactivation can be described in terms of "formation of a stable intermediate" which is hydrolyzed under alkaline conditions.[27] The intermediate is most likely an acyl-antibody resulting from nucleophilic attack by amino acid residue(s) in or near the combining site of **1g**. In consideration of recent efforts to detect acyl-antibody using ion spray mass spectrometry[28] or isoelectric focusing analysis,[29] the present finding is significant and provides an alternative approach.[30]

Thus the present analysis of antibody inactivation revealed an acyl-intermediate-mediated multistep kinetic sequence for the hydrolytic reaction of 4A1, which involves rapid formation of an acyl intermediate, followed by its hydrolysis.[31] A plausible mechanism is shown in Fig. 6. The inactivation of 4A1 antibody in the hydrolysis of substrate **1g** can be explained by conversion of the covalent acyl-antibody formed with **1g** to a much less active conformational state against direct attack by hydroxide. As a result, subsequent deacylation by hydroxide ion becomes much slower than acylation ($k_2 >> k_3$),[32] so that the activity of the catalytic antibody significantly decreases after a few turnovers.

On the contrary, substrate **1d** maintained remarkable rate acceleration during many turnovers without slowing the reaction velocity. It indicates that the acyl-antibody formed with **1d** is hydrolyzed easily after the acylation.[26] Although both substrates **1d** and **1g** demonstrate high initial velocity, those are different in terms of the reactivity against hydroxide.[33] In order to design an optimum substrate, the difference needs to be clarified.

To date, two approaches toward improving catalytic efficiency (k_{cat}/k_{uncat}) with substrate tolerance have been demonstrated successfully. One is to create antibody-substrate destabilization via weaker substrate binding, manifested by an increase in K_m.[10,34] However, the specificity constant (k_{cat}/K_m), one of the most essential properties of a biocatalyst, is sacrificed for elevation of the apparent catalytic efficiency (k_{cat}/k_{uncat}) in this approach.[35] The other is to introduce a nonspecificity element with a strong immunogenic moiety in the hapten molecule.[17]

Interestingly, 4A1 antibody also appears to tolerate a variety of substituents in the proximal region, as seen in the side chains of **1c—1f**. It should be emphasized that the substrate tolerance observed in 4A1 antibody does not accompany a significant increase in K_m value. Consequently, high values of the specificity constant (k_{cat}/K_m) are obtained with alternate substrates.[35] Recently a similar tendency has been observed in the antibody catalyzed Kemp elimination reaction.[36] This suggested that the antibody pocket is relatively open in the vicinity of the substituents and makes no steric demands on the substrate in this region. These results indicate that substrate alteration in the carrier-proximal region may provide new avenues to design substrates in order to expand the window for substrates with high catalytic activity.[37]

It is generally thought that the specificity of catalytic antibodies, although not always predictable, is affected mostly by the more exposed, more immunogenic, carrier-distal portion of the hapten.[17] However, recent X-ray crystallographic studies have indicated that at least 90% of the hapten molecule is deeply buried in the combining site with the *p*-nitrophenyl group at the bottom of the pocket and the carrier-proximal aliphatic region toward the surface.[32,38—40] Considering the size of the antigen-binding site (700—800 Å), One might expect that any given haptenic structure would induce an antibody molecule exhibiting a specific activity pattern against the carrier-proximal side chain in the substrate. Indeed the competitive ELISA using BSA-hapten conjugate displayed the highest affinity constant (K_d) of 6×10^{-7} M for phosphate **2d**, a transition-state analog of **1d**, indicating that the side chain of the substrate **1d** enables strong interaction with 4A1 antibody's binding site. Moreover, chemical modification studies and computer-assisted model building of V region of 4A1 antibody demonstrated that Arg residue near the surface of the 4A1 antibody's binding site is likely to be involved in interaction with the side chain of substrate **1d** and **1g**.[19,41]

Finally, characterization of the 4A1 catalytic antibody provides an alternative approach to the design of optimal substrates for hydrolytic reaction. This study also offers important tools for mechanistic analysis of the enzymatic nature of catalytic antibodies.

The authors thank Mr. Mitsuo Yoshikane for carrying out the 600 MHz ^{13}C NMR work and Ms. Haruko Shimizu for technical assistance.

References

1) For this series, see Refs. 18 and 19.

2) W. P. Jencks, "Catalysis in Chemistry and Enzymology," McGraw-Hill, New York (1969).

3) S. J. Pollack, J. W. Jacobs, and P. G. Schultz, *Science*, **234**, 1570 (1986).

4) A. Tramontano, K. D. Janda, and R. A. Lerner, *Science*, **234**, 1566 (1986).
5) P. G. Schultz and R. A. Lerner, *Science*, **269**, 1835 (1995).
6) A. J. Kirby, *Acta Chem. Scand.*, **50**, 203 (1996).
7) J. R. Jacobsen and P. G. Schultz, *Curr. Opin. Struct. Biol.*, **5**, 818 (1995).
8) D. S. Tawfik, Z. Eshhar, and B. S. Green, *Mol. Biotechnol.*, **1**, 87 (1994).
9) L. C. Hsieh, S. Yonkovich, L. Kochersperger, and P. G. Schultz, *Science*, **260**, 337 (1993).
10) K. D. Janda, S. J. Benkovic, D. A. McLeod, D. M. Schloeder, and R. A. Lerner, *Tetrahedron*, **47**, 2503 (1991).
11) Y. Iwabuchi, H. Miyashita, R. Tanimura, K. Kinoshita, M. Kikuchi, and I. Fujii, *J. Am. Chem. Soc.*, **116**, 771 (1994).
12) B. L. Iverson, K. E. Cameron, G. K. Jahangiri, and D. S. Pasternak, *J. Am. Chem. Soc.*, **113**, 5320 (1990).
13) A. Tramontano, A. A. Ammann, and R. A. Lerner, *J. Am. Chem. Soc.*, **110**, 2282 (1988).
14) K. D. Janda, J. A. Ashley, T. M. Jones, D. A. McLeod, D. M. Schloeder, M. I. Weinhouse, R. A. Lerner, R. A. Gibbs, P. A. Benkovic, R. Hilhorst, and S. J. Benkovic, *J. Am. Chem. Soc.*, **113**, 291 (1991).
15) M. K. Shokat and P. G. Schultz, *Methods Enzymol.*, **203**, 327 (1991).
16) J. Jacobs and P. G. Schultz, *J. Am. Chem. Soc.*, **109**, 2174 (1987).
17) T. Li, S. Hilton, and K. D. Janda, *J. Am. Chem. Soc.*, **117**, 2123 (1995).
18) Y. Wada, M. Yamamoto, I. Itoh, and M. Ono, *Chem. Lett.*, **1997**, 1223.
19) Y. Wada, Y. Sudo, and M. Ono, *Chem. Lett.*, **1997**, 1225.
20) S. E. Szedlacsek and R. G. Duggleby, *Methods Enzymol.*, **249**, 144 (1995).
21) K. D. Janda, M. I. Weinhouse, T. Danon, K. A. Pacelli, and D. M. Schloder, *J. Am. Chem. Soc.*, **113**, 5427 (1991).
22) M. T. Martin, A. D. Napper, P. G. Schultz, and A. R. Rees, *Biochemistry*, **30**, 9757 (1991).
23) K. D. Janda, R. A. Lerner, and A. Tramontano, *J. Am. Chem. Soc.*, **10**, 4835 (1988).
24) K. D. Janda, S. J. Benkovic, and R. A. Lerner, *Science*, **244**, 437 (1989).
25) G. R. Nakayama and P. G. Schultz, *J. Am. Chem. Soc.*, **114**, 780 (1992).
26) J. D. Stewart, J. F. Krebs, G. Siuzdak, A. J. Berdis, D. B. Smithrud, and S. J. Benkovic, *Proc. Natl. Acad. Sci. U.S.A.*, **91**, 7404 (1994).
27) D. S. Tawfik, R. R. Zemel, R. Arad-Yellin, B. S. Green, and Z. Eshhar, *Biochemistry*, **29**, 9916 (1990).
28) J. F. Krebs, G. Siuzdak, H. J. Dyson, J. D. Stewart, and S. J. Benkovic, *Biochemistry*, **34**, 720 (1995).
29) B. Gigant, J-B. Charbonnier, B. Golinelli-Pimpaneau, R. R. Zemel, Z. Eshhar, B. S. Green, and M. Knossow, *Eur. J. Biochem.*, **246**, 471 (1997).
30) J. Guo, W. Huang, and T. S. Scanlan, *J. Am. Chem. Soc.*, **116**, 6062 (1994).
31) S. J. Benkovic, J. A. Adams, C. L. Borders, K. D. Janda, and R. A. Lerner, *Science*, **250**, 1135 (1990).
32) B. Gigant, J-B. Charbonnier, Z. Eshhar, B. S. Green, and M. Knossow, *Proc. Natl. Acad. Sci. U.S.A.*, **94**, 7857 (1997).
33) R. Zemel, D. G. Schindler, D. S. Tawfik, Z. Eshhar, and B. S. Green, *Mol. Immnol.*, **31**, 127 (1994).
34) I. Fujii, R. A. Lerner, and K. D. Janda, *J. Am. Chem. Soc.*, **113**, 8528 (1991).
35) R. A. Gibbs, P. A. Benkovic, K. D. Janda, R. A. Lerner, and S. J. Benkovic, *J. Am. Chem. Soc.*, **114**, 3528 (1992).
36) A. G-Grandpierre and C. Teiller, *Bioorg. Med. Chem. Lett.*, **7**, 2497 (1997).
37) L. C. Hsieh, J. C. Stephans, and P.G. Schultz, *J. Am. Chem. Soc.*, **116**, 2167 (1994).
38) J-B. Charbonnier, E. Carpenter, B. Gigant, B. Golinelli-Pimpaneau, Z. Eshhar, B. S. Green, and M. Knossow, *Proc. Natl. Acad. Sci. U.S.A.*, **92**, 11721 (1995).
39) P. A. Patten, N. S. Gray, P. L. Yang, C. B. Marks, G. J.Wedemayer, J. J. Boniface, R. C. Stevens, and P. G. Schultz, *Science*, **271**, 1086 (1996).
40) G. W. Zhou, J. Guo, W. Huang, R. J. Fletterick, and T. S. Scanlan, *Science*, **265**, 1059 (1994).
41) H. Suzuki, E. B. Mukouyama, C. Wada, Y. Kawamura-Konishi, Y. Wada, and M. Ono, *J. Protein Chem.*, **17**, 273 (1998).